Pure Appl. Chem., Vol. 83, No. 11, pp. 2055–2062, 2011.
doi:10.1351/PAC-CON-11-04-05

Novel nanochemistry toward generation and stabilization of gold nanoparticles in human serum albumin matrix*

Raghuraman Kannan‡, Satish Nune, Nripen Chanda, Ajit Zambre, and Ravi Shukla

Department of Radiology, Room #106, Alton Building Laboratories, 301 Business loop 70W, University of Missouri, Columbia, MO 65211, USA

Abstract: The interactions of gold nanoparticles (AuNPs) with human serum albumin (HSA) greatly influence their in vivo characteristics. It is important to develop conjugates that can serve as ideal structural models to understand the interaction of AuNPs with HSA. We report the synthesis and stabilization of AuNPs in HSA matrix with no additional ligands on the surface of the NPs. The hydrodynamic size of the AuNP–HSA conjugate is 22 nm, and transmission electron microscopy (TEM) measurement shows the core size as 8–13 nm. We have performed strip assay to establish that the biological activity of HSA is retained even after conjugation. Our cellular toxicity evaluation studies show that AuNP–HSA conjugates are nontoxic and biocompatible.

Keywords: dynamic light scattering (DLS); gold; human serum albumin (HSA); inorganic chemistry; nanoparticles; transmission electron microscopy (TEM).

INTRODUCTION

Nanoparticles (NPs) are being tested for myriad applications in the field of medicine [1–8]. Some of the recent studies confirm that tailored NPs cross membranes and enhance diagnostic imaging techniques to provide greater details on specific biological processes [9–11]. Among various metallic NPs, gold nanoparticles (AuNPs) possess many of the vital attributes required for in vivo medical applications. Hybrid AuNPs have been generated by surface-conjugating AuNPs with antibody, peptide, or small molecules to impart target specificity under in vivo conditions [12–15]. However, under in vivo conditions, NPs interact and coat with serum proteins over the surface, leading to the formation of corona [15]. The formation of corona strongly depends on the size, surface charge, and the molecules coated over the surface of the NPs [15]. On the other hand, serum proteins upon interaction with NPs undergo both structural and conformational change [16]. The in vivo properties of the NPs strongly depend on the nature of interaction with serum proteins [17]. Previous studies have mainly focused on the interaction (or coating) of serum proteins over the biomolecule-conjugated NPs [17]. These biomolecules have a defined biological half-life and decompose to smaller molecules through metabolic processes and eventually unlink from the metallic core. At this stage, the bare metallic core (or naked NP) is exposed to blood proteins (Fig. 1 describes schematically the nature of NPs under in vivo conditions).

*Paper based on a presentation made at the International Conference on Nanomaterials and Nanotechnology (NANO-2010), Tiruchengode, India, 13–16 December 2010. Other presentations are published in this issue, pp. 1971–2113.

‡Corresponding author

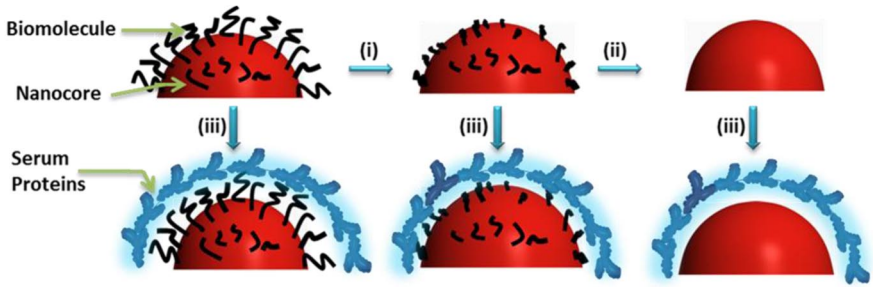

Fig. 1 Schematic representation of interaction of hybrid NPs with blood proteins. (i) Disintegration of biomolecule in hybrid nanoparticles; (ii) complete removal of biomolecule from the nanocore; (iii) interaction of serum proteins with nanoparticles.

In comparison, the structural changes on the serum proteins imparted by this process would be significantly different than the coating of serum proteins over the surface of the bare NPs. Nevertheless, our knowledge base on the nature of interaction of serum proteins with bare metallic nanocores is scanty. Undoubtedly, the reason for the paucity of such a study is due to the inherent instability of NPs in plasma proteins toward aggregation. Therefore, there is a strong rationale for developing simulated nanocore structures, truly representing the nature of AuNPs in the presence of serum blood proteins. Specifically, our studies are focused on developing AuNP–human serum albumin (HSA) matrix with no additional ligands or biomolecules on the surface of the NPs and investigating in vitro characteristics. The reason for choosing HSA is centered on the fact that the interaction of pharmaceuticals with HSA is considered to be crucial in determining the in vivo activity of the drug. HSA is one of the major ingredients in plasma proteins (up to 60 %) [17] and is the most abundant protein in the circulatory system; it is highly capable of binding various biomolecules ranging from metabolites, drugs, and organic compounds to metallic or non-metallic NPs [17]. In fact, in vivo plasma Au distribution studies of a Au-based rheumatoid arthritis drug in human patients revealed that 85–95 % of Au is bound to albumin [18,19]. The results reported in this research article include: (i) synthesis and characterization of AuNP–HSA conjugates, (ii) in vitro stability studies of AuNP–HSA conjugates toward various biologically relevant biomolecules, and (iii) biological activity and in vitro cellular toxicity of AuNP–HSA conjugates.

MATERIALS AND METHODS

General

The components used in the synthesis of AuNPs were procured from standard vendors: HSA from Aldrich, $NaAuCl_4$ from Alfa-Aesar. Transmission electron microscopy (TEM) images were obtained on JEOL 1400 TEM, JEOL, Ltd., Tokyo, Japan. TEM samples were prepared by placing 5 μL of AuNP solution on the 300 mesh carbon-coated copper grid and allowed the solution to sit for 5 min; excess solution was removed carefully, and the grid was allowed to dry for an additional 5 min. The average size and size distribution of AuNPs synthesized were determined by the processing of the TEM image using image processing software such as Adobe Photoshop (with Fovea plug-ins). UV–vis spectroscopy: The absorption measurements were done using Varian Cary50 UV–vis spectrophotometers with 1 mL of AuNP solution in disposable cuvettes of 10 mm path length.

Synthesis of AuNP–HSA conjugates

To a 20 mL vial was added 10 mL of doubly ionized (DI) water, followed by the addition of 50 mg of HSA and 6.4 mg of $P(CH_2NHCH(CH_3)COOH)_3$ (THPAL). The reaction mixture was stirred continuously at 25 °C for 2 min. To the stirring mixture was added 15 mg of $NaAuCl_4$ solution (in DI water; 2 mL). The color of the mixture turned purple–red from pale yellow within 5 min after the addition, indicating the formation of AuNPs. The reaction mixture was allowed to stir for additional 2 h. The AuNPs thus formed were characterized by UV–vis absorption spectroscopy and TEM analysis.

In vitro stability studies

In vitro stability of the serum-coated AuNPs was tested in the presence of NaCl, cysteine, histidine, HSA, and bovine serum albumin (BSA) solutions. Typically, 1 mL of AuNP solution was added to glass vials containing 0.5 ml of 10 % NaCl, 0.5 % cysteine, 0.2 M histidine, 0.5 % HSA and BSA solutions, respectively, and incubated for 30 min. We also have studied the in vitro stability with various phosphate buffers (pH 7 and 9) following the above similar procedure. The stability and identity of the NPs were measured by recording UV absorbance at 0.5 h as well as after 16 h. The surface plasmon resonance band at 530 nm confirmed the retention of nanoparticulates in all the above mixtures. TEM measurements inferred the retention of the nanoparticulate compositions, signifying the robust nature of these NPs under in vitro conditions.

Effect of dilution

The detailed investigation to ascertain the effect of dilution of AuNP–HSA conjugate was performed in order to establish the stability of AuNP–HSA by monitoring the plasmon resonance wavelength (λ_{max}) after every successive addition of 0.2 mL of DI water to 1 mL of AuNP solutions. The absorption intensity at λ_{max} is found to be linearly dependent on the concentration of AuNPs, in accordance with Beer–Lambert's law. It is important to recognize that λ_{max} of AuNPs did not change at very dilute conditions. These are typical concentrations encountered when working at cellular levels.

Strip assay

To 1.0 μL of different concentrations anti-human serum antibody (sigma) was spotted on a 1 × 6 cm nitrocellulose membrane strip. The membrane was air-dried, and non-specific sites on the membrane were blocked for 2 h at 25 °C using blocking buffer with 2 % skimmed milk in 1 × phosphate buffered saline containing 0.02 % triton-X 100. After blocking, the strip was washed and incubated with 0.06 mg/mL pre-washed AuNP–HSA. Development of a ruby red color after 3 h at 25 °C at place of spotted antibody was an indication of the HSA–antibody interaction and hence the biological activity of HSA post-conjugation.

In vitro cytotoxicity measurements (MTT assay)

Fibroblast cells were maintained in DMEM with 10 pg/mL^{-1} phenol red, 10 mM HEPES, 100 units mL^{-1} penicillin, 100 pg/mL^{-1} streptomycin, and 10 % donor bovine serum (maintenance medium). The in vitro cytotoxicity evaluation of HSA-coated AuNPs was performed as described by the supplier (ATCC, USA). Briefly, 2×10^4 fibroblast cells at the exponential growth phase were seeded in each well of a flat-bottomed 96-well polystyrene-coated plate and were incubated at 37 °C for 24 h in CO_2 incubator at 5 % CO_2 environment. A series of dilutions like 0, 5.5, 11, 16.5, 22, 27.5, and 33 μg/mL concentrations of AuNP–HSA (Au atoms) were made in the medium. Each concentration was added to the plate in a pentaplet manner. After 24 h incubation, 10 μL per well MTT [3-(4,5-dimethylthiazol-2-yl)-

2,5-diphenyltetrazolium bromide] (stock solution 5 mg/mL^{-1} PBS) (ATCC, USA) was added for 24 h, and formosan crystals so formed were dissolved in 100 µL detergent. The plates were kept for 18 h in dark at 25 °C to dissolve all the crystals, and the intensity of the developed color was measured by microplate reader (Dynastic MR 5000, USA) operating at 570 nm wavelength. Wells with complete medium, NPs, and MTT, but without cells were used as blanks. Untreated cells were considered 100 % viable.

RESULTS AND DISCUSSION

In order to understand the physicochemical characteristics of Au–albumin conjugates, the following requirements need to be fulfilled: (i) a simulated naked nanocore should be attached directly to albumin proteins with no molecular linker in between metal core and albumin; (ii) the naked nanocore should have surface contact only with the albumin proteins; and (iii) the nanocore should have moderate stability under in vitro conditions.

Synthesis of AuNP–HSA conjugates

Our synthetic protocol involves the simple addition of sodium tetrachloroaurate solution ($NaAuCl_4$) in aqueous media to the stirring aqueous solution of HSA (0.5 %, 50 mg in 10 mL DI water) and a non-toxic phosphino amino acid [$P(CH_2NHCH(CH_3)(COOH)_3$]; THPAL] [20,21] at 25 °C. Addition of gold salt resulted in the formation of AuNPs within 2 h with over 98 % yield at 25 °C. Absorption measurements indicated that the plasmon resonance wavelength, λ_{max} of AuNP–HSA is ~530 nm. The sizes of AuNP–HSA are in the range of 8–13 nm as measured from TEM techniques (Fig. 2). It is presumed that the disulfides in the HSA effectively stabilized the NPs to provide excellent robustness against agglomeration [13,14]. Our reaction methodology involves the utilization of mild reducing agent THPAL that will help in the reduction of only Au(III) to AuNPs and not the biogenic chemical functionalities present on serum proteins, thus retaining the overall biospecificity of HSA [20,21]. In an aim to obtain and study the library of AuNPs of different sizes with various stabilizers for our studies, we further developed AuNP–HSA.

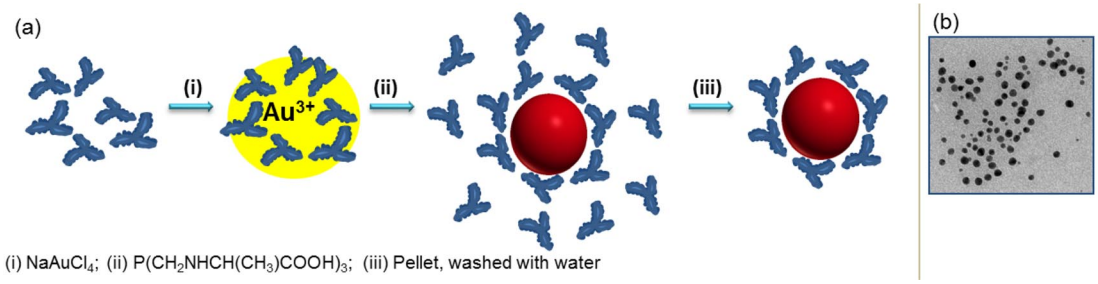

Fig. 2 (a) Synthesis of AuNP–HSA conjugates; (b) TEM image of AuNP–HSA conjugate.

NP size characterization and size distribution

Physicochemical properties, such as size, charge, and morphology of AuNPs generated using HSA, were determined by TEM and dynamic light scattering (DLS) methods. TEM determines the core size of AuNPs, and DLS was used to evaluate the size of HSA-coated gold. TEM measurements on AuNP–HSA showed that particles are spherical in shape within the size range of 8–13 nm. Size distribution analysis of AuNP–HSA confirms that particles are mono disperse and uniform (Fig. 2). We also

employed a DLS method (hydrodynamic radius) to confirm the presence of serum proteins on the surface of AuNPs. The serum protein coatings on AuNPs are expected to cause substantial changes in the hydrodynamic radius of AuNP–HSA. The hydrodynamic diameter of AuNP–HSA as determined from DLS measurements is 22 ± 1 nm, suggesting that serum proteins are capped on AuNPs. DLS studies of the AuNPs revealed an increase in the hydrodynamic diameter as the serum proteins form the monolayer. The measurement of charge on NPs, zeta-potential (ζ), provides crucial information on the stability of the NP dispersion [22–25]. The magnitude of the measured ζ is an indication of the repulsive forces that are present and can be used to predict the long-term stability of the nanoparticulate dispersion. The stability of nanoparticulate dispersion depends upon the balance of the repulsive and attractive forces that exist between NPs as they approach one another. If all the particles have a mutual repulsion then the dispersion will remain stable. However, little or no repulsion between particles leads to aggregation. The positive ζ of 29 ± 2 mV for AuNP–HSA indicates that the particles repel each other and there is no tendency for the particles to aggregate.

In vitro stability studies

To understand the stability of AuNP–HSA conjugates under biologically relevant conditions, we treated AuNP–HSA conjugates with 10 % NaCl, 0.5 % cysteine, 0.2 M histidine, 0.5 % BSA, or 0.5 % HSA solutions and monitored λ_{max} of the resultant mixture (Fig. 3). The plasmon wavelength and width in all the above formulations shifts ~5 nm. This indicates that the AuNPs are intact and, thus, demonstrate the high in vitro stability of AuNP–HSAs in biological fluids at physiological pH. It is noteworthy that the NPs coated with serum proteins are stable even when they are challenged with high ionic strength solutions such as 10 % NaCl. It is well known that the addition of certain peptides or proteins to AuNPs may decrease their stabilities to salt solutions appreciably. Our results are also further corroborated by the recent report on the critical flocculation concentrations of peptide-AuNPs [26].

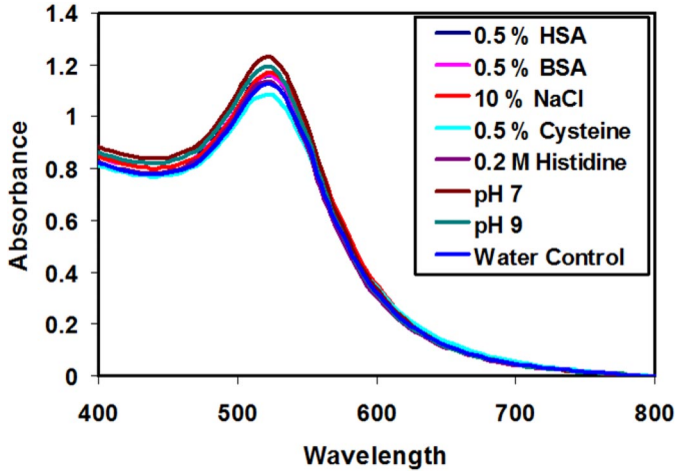

Fig. 3 In vitro stability studies of AuNP–HSA by monitoring UV–vis absorption peak at ~540 nm wavelength.

We next investigated the change in physicochemical characteristics of AuNP–HSA conjugates in various different concentrations. In order to establish the stability of AuNP–HSA under dilution, the plasmon resonance wavelength (λ_{max}) was monitored after every successive addition of 0.2 mL of DI water to 1 mL of AuNP solutions. It is important to recognize that λ_{max} of AuNPs did not change at dilutions in the range of 10^{-5}–10^{-6} M. These are typical concentrations encountered when working at

cellular levels. These data clearly confirm that serum-coated AuNPs are highly stable in solutions of NaCl, cysteine, histidine, HSA, and BSA. It is conceivable that the interaction between disulfide structure contained within serum protein backbone with Au atoms provides extraordinary in vitro stability.

HSA-bioactivity studies: Strip assay

Earlier reports have shown that AuNPs self-assemble in HSA matrix, leading to the formation of hollow spheres [27]. It is perceived that formation of such a self-assembly would lead to the destruction of biological activity of HSA. In order to assess whether the biological activity of HSA is affected during AuNP–HSA conjugation in terms of HSA binding to a specific antibody, we performed a strip assay wherein HSA-specific polyclonal antibody was probed as HSA-conjugated AuNPs. For this study, 1 µL of increased concentrations of anti-HSA were placed in a nitrocellulose membrane strip. The non-specific sites of the membrane were blocked by using milk protein. The whole strip was then incubated with 0.06 mg/mL pre-washed AuNP–HSA for 3 h. During the incubation time, the AuNP–HSA entered into the matrix of the strip, formed complex between anti-HSA and Au-conjugated HSA and saturated the spots in a circular manner, as shown in Fig. 4. The concept of the immunoassay is to have an immobilized antibody (anti-HSA) zone in the membrane strip that is exposed to the target antigen conjugated with AuNP (AuNP–HSA) in the solution. The formation of circular red spots was indicative of HSA–antibody interaction and hence the biological activity of HSA post-conjugation. The intensity of the spots was proportional to the concentration of the proteins used in this study [28]. Our studies reveal that HSA is biologically active and the property of the resultant AuNP–HSA will be largely influenced by the HSA matrix and not by the Au core.

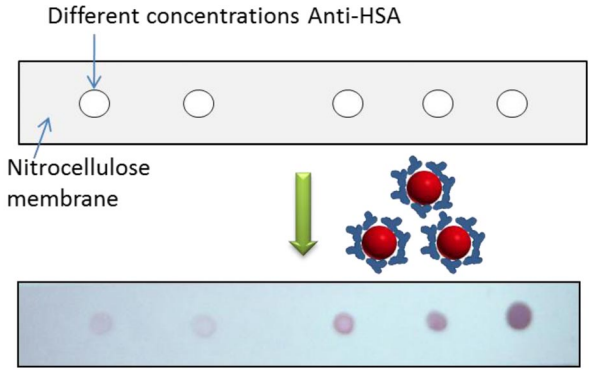

Fig. 4 Strip assay of HSA-conjugated AuNPs toward anti-HSA antibody. The intensity of the spots was increased with increasing concentrations of the proteins.

Toxicity of nanoparticles: MTT studies

AuNPs have shown promising applications in the area of biomedical imaging and therapy. The potential concentrations at which they might be used for developing a biomedical imaging agent could be toxic. Moreover, the stability of AuNPs at reasonably high concentration becomes increasingly important under in vivo conditions. We have already investigated the stability of the AuNP–HSA in different biological mediums and hypothesized that the serum proteins presumably influence the overall stability and might lead to contemplating their biocompatibility evaluation based on their potential cytotoxicity. We have studied the cytotoxicity of AuNP–HSA using normal fibroblast cell cultures as in vitro by the MTT assay. The cells were treated with 0, 5.5, 11, 16.5, 22, 27.5, and 33 µg/mL concentrations of AuNP–HSA for 24 h and were subjected to the MTT assay for cell-viability determination. After

24 h of AuNP–HSA treatment, cells showed more than 85 % viability up to 33 μg/mL concentrations (Fig. 5). This result clearly demonstrates that AuNP–HSA do not show any detectable cytotoxicity up to 33 μg/mL concentrations of Au atoms in fibroblast cells.

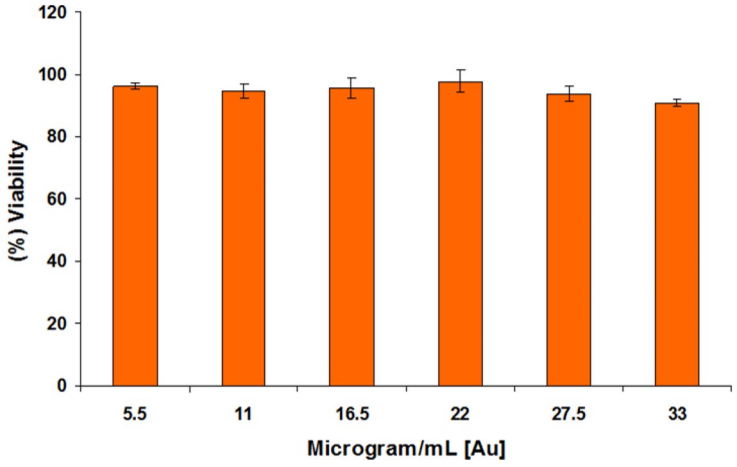

Fig. 5 Cell viability of fibroblast cells after 24 h of incubation with increasing amounts of AuNP–HSA showing nontoxic profiles.

CONCLUDING REMARKS

In conclusion, spherical AuNPs coated with HSA have been synthesized in a single step, using a nontoxic phosphorus-containing compound as the reducing agent. We investigated the particle size and stability of Au–HSA in the presence of NaCl, cysteine, histidine, HSA, BSA, and different pH. Our results confirmed that the NPs have biocompatible properties such as nontoxicity without disturbing cell functionality, which could be beneficial for biomedical applications.

REFERENCES

1. R. R. Arvizo, S. Rana, O. R. Miranda, R. Bhattacharya, V. M. Rotello, P. Mukherjee. *Nanomedicine* (2011). doi:10.1016/j.nano.2011.01.011
2. H. Wang, L. Zheng, C. Peng, R. Guo, M. Shen, X. Shi, G. Zhang. *Biomaterials* **32**, 2979 (2011).
3. M. Patlak. *J. Natl. Cancer Inst.* **103**, 173 (2011).
4. K. K. Jain. *BMC Med.* **8**, 83 (2010).
5. S. Bhattacharyya, R. A. Kudgus, R. Bhattacharya, P. Mukherjee. *Pharm. Res.* **28**, 237 (2011).
6. J. Xie, S. Lee, X. Chen. *Adv. Drug Delivery Rev.* **62**, 1064 (2010).
7. D. A. Giljohann, D. S. Seferos, W. L. Daniel, M. D. Massich, P. C. Patel, C. A. Mirkin. *Angew. Chem., Int. Ed. Engl.* **49**, 3280 (2010).
8. E. Boisselier, D. Astruc. *Chem. Soc. Rev.* **38**, 1759 (2009).
9. E. C. Cho, C. Glaus, J. Chen, M. J. Welch, Y. Xia. *Trends Mol. Med.* **16**, 561 (2010).
10. M. Seo, I. Gorelikov, R. Williams, N. Matsuura. *Langmuir* **26**, 13855 (2010).
11. S. E. Skrabalak, L. Au, X. Lu, X. Li, Y. Xia. *Nanomedicine* **2**, 657 (2007).
12. T. Stuchinskaya, M. Moreno, M. J. Cook, D. R. Edwards, D. A. Russell. *Photochem. Photobiol. Sci.* **10**, 822 (2011).

13. N. Chanda, V. Kattumuri, R. Shukla, A. Zambre, K. Katti, A. Upendran, R. R. Kulkarni, P. Kan, G. M. Fent, S. W. Casteel, C. J. Smith, E. Boote, J. D. Robertson, C. Cutler, J. R. Lever, K. V. Katti, R. Kannan. *Proc. Natl. Acad. Sci. USA* **107**, 8760 (2010).
14. N. Chanda, R. Shukla, K. V. Katti, R. Kannan. *Nano Lett.* **9**, 1798 (2009).
15. I. Lynch, K. A. Dawson. *Nano Today* **3**, 40 (2008).
16. (a) D.-H. Tsai, F. W. DelRio, A. M. Keene, K. M. Tyner, R. I. MacCuspie, T. J. Cho, M. R. Zachariah, V. A. Hackley. *Langmuir* **27**, 2464 (2011); (b) A. Kunzmann, B. Andersson, T. Thurnherr, H. Krug, A. Scheynius, B. Fadeel. *Biochim. Biophys. Acta* **1810**, 361 (2011).
17. (a) K. Ohnishi, A. Kawaguchi, S. Nakajima, H. Mori, T. Ueshima. *J. Clin. Pharmacol.* **48**, 203 (2008); (b) M. Fasano, S. Curry, E. Terreno, M. Galliano, G. Fanali, P. Narciso, S. Notari, P. Ascenzi. *IUBMB Life* **57**, 787 (2005).
18. R. J. van de Stadt, B. Abbo-Tilstra. *Ann. Rheum. Dis.* **39**, 31 (1980).
19. S. M. Pedersen. *Ann. Rheum. Dis.* **45**, 712 (1986).
20. R. Kannan, V. Rahing, C. Cutler, R. Pandrapragada, K. K. Katti, V. Kattumuri, J. D. Robertson, S. J. Casteel, S. Jurisson, C. Smith, E. Boote, K. V. Katti. *J. Am. Chem. Soc.* **128**, 11342 (2006).
21. V. Kattumuri, K. Katti, S. Bhaskaran, E. J. Boote, S. W. Casteel, G. M. Fent, D. J. Robertson, M. Chandrasekhar, R. Kannan, K. V. Katti. *Small* **3**, 333 (2007).
22. N. Chanda, R. Shukla, A. Zambre, S. Mekapothula, R. R. Kulkarni, K. Katti, K. Bhattacharyya, G. M. Fent, S. W. Casteel, E. J. Boote, J. A. Viator, A. Upendran, R. Kannan, K. V. Katti. *Pharm. Res.* **28**, 279 (2011).
23. E. Boote, G. Fent, V. Kattumuri, S. Casteel, K. Katti, N. Chanda, R. Kannan, R. Churchill. *Acad. Radiol.* **17**, 410 (2010).
24. S. K. Nune, N. Chanda, R. Shukla, K. Katti, R. R. Kulkarni, S. Thilakavathi, S. Mekapothula, R. Kannan, K. V. Katti. *J. Mater. Chem.* **19**, 2912 (2009).
25. N. Chanda, P. Kan, L. D. Watkinson, R. Shukla, A. Zambre, T. L. Carmack, H. Engelbrecht, J. R. Lever, K. Katti, G. M. Fent, S. W. Casteel, C. J. Smith, W. H. Miller, S. Jurisson, E. Boote, J. D. Robertson, C. Cutler, M. Dobrovolskaia, R. Kannan, K. V. Katti. *Nanomedicine* **6**, 201 (2010).
26. H. Xie, A. Tkachento, W. R. Glomm, J. A. Ryan, M. K. Brennaman, J. M. Papanikas, S. Franzen, D. L. Feldheim. *Anal. Chem*. **75**, 5797 (2003).
27. N. C. Nayak, K. Shin. *Nanotechnology* **19**, 265603 (2008).
28. Z. Afrasiabi, R. Shukla, N. Chanda, S. Bhaskaran, A. Upendran, A. Zambre, K. V. Katti, R. Kannan. *J. Nanosci. Nanotechnol.* **10**, 719 (2010).

